Japanese Journal of Applied Physics **56**, 07JF01 (2017)
https://doi.org/10.7567/JJAP.56.07JF01

REGULAR PAPER

Imaging of human vertebral surface using ultrasound RF data received at each element of probe for thoracic anesthesia

Kazuki Takahashi[1*], Hirofumi Taki[1,2], Eiko Onishi[3], Masanori Yamauchi[3], and Hiroshi Kanai[2,1]

[1]*Graduate School of Biomedical Engineering, Tohoku University, Sendai 980-8579, Japan*
[2]*Graduate School of Engineering, Tohoku University, Sendai 980-8579, Japan*
[3]*Department of Anesthesiology and Perioperative Medicine, Tohoku University School of Medicine, Sendai 980-8575, Japan*

*E-mail: kanai@ecei.tohoku.ac.jp

Received November 25, 2016; accepted February 6, 2017; published online May 23, 2017

Epidural anesthesia is a common technique for perioperative analgesia and chronic pain treatment. Since ultrasonography is insufficient for depicting the human vertebral surface, most examiners apply epidural puncture by body surface landmarks on the back such as the spinous process and scapulae without any imaging, including ultrasonography. The puncture route to the epidural space at thoracic vertebrae is much narrower than that at lumber vertebrae, and therefore, epidural anesthesia at thoracic vertebrae is difficult, especially for a beginner. Herein, a novel imaging method is proposed based on a bi-static imaging technique by making use of the transmit beam width and direction. In an in vivo experimental study on human thoracic vertebrae, the proposed method succeeded in depicting the vertebral surface clearly as compared with conventional B-mode imaging and the conventional envelope method. This indicates the potential of the proposed method in visualizing the vertebral surface for the proper and safe execution of epidural anesthesia.

1. Introduction

Epidural anesthesia is a type of regional anesthesia without loss of consciousness, used to produce anesthetic effects in an optional range below the neck. Especially, it has been reported that 60% of American women in 27 states who experienced a single birth received epidural or spinal anesthesia,[1)] and it is reported that epidural anesthesia was employed for lower limb surgery longer than 2 h in 57 of 148 hospitals (39%) in Japan.[2)] Epidural anesthesia has the following advantages compared with general anesthesia or opioid analgesics: superior effects against pain with movement, gastrointestinal peristalsis and blood circulation, and fewer systemic side effects.[3)] Respiratory complications such as atelectasis and pneumonia are less than those with opioid use, and the function of the gastrointestinal tract, blood circulation and wound healing can recover faster than without epidural anesthesia due to the sympathetic nerve blocking effects. Consequently, continuous epidural anesthesia using a catheter is a common technique for perioperative analgesia and an effective treatment for early postoperative recovery.

In epidural anesthesia, as shown Fig. 1(a), an examiner advances an anesthetic needle to the epidural space located at the outer layer of the dura mater. The needle tip does not always straightly obtain the epidural space, and dorsal bone structures, namely, the spinous process and the vertebral arch, sometimes block the needle. Moreover, measurements of the width of the epidural space and observation of epidural fluid or abscess is needed to perform safe epidural puncture or prevent post-puncture complications, such as paresis or post-dura puncture headache due to hematoma or outflux of the cerebrospinal fluid, respectively.

For imaging the internal human body, computed tomography (CT) and magnetic resonance imaging (MRI) are employed. However, CT has a risk of radiation exposure, and MRI has disadvantages in that the scale of the equipment is large and measurement time is long. Since non-invasive, iterative diagnosis and short-time measurement are possible, ultrasound measurement is one of the main methods of in vivo imaging, and some studies have suggested its usefulness.[4–7)]

Although an examiner often confirms an ultrasound image before the application of epidural puncture,[8)] it is still difficult to advance an epidural needle with real-time ultrasound guidance because the structure of vertebrae is complex. Previously, imaging of the human radius surface using phase symmetry[9)] and an automatic classification of epidural space and the vertebral arch have been studied.[10–12)] However, ultrasound imaging is difficult when the target, such as the thoracic surface, has a complex shape. Especially, in the thoracic area, as shown in Fig. 1(b), spinous processes and the vertebral arch are extended caudally, but the thoracic window to access the epidural space is much narrower than that in the cervical or lumbar region.[13)] The narrow acoustic window to observe the epidural space in the thoracic area limits the ultrasound depiction of this space.[14)] Since spinous processes and the vertebral arch prevent easy advancement of the puncture to the epidural space, the task of anesthesiologists would be facilitated by auxiliary imaging with easy and noninvasive techniques.

Conventional B-mode imaging is an easy and noninvasive technique to depict the spinal surface. In conventional B-mode imaging, since the direction of the receive beam and that of the transmit beam are the same, the surface should be perpendicular to the ultrasound beam. However, the bone surface is smooth and the received signal is severely decreased when the ultrasound beam is not perpendicular to the surface. Therefore, ultrasonography is insufficient for depicting the vertebral surface, and successful administration of epidural anesthesia depends on the examiner's experience and ability of locating a gap between vertebrae by touch. The failure rate of epidural anesthesia has been reported to be 6–25%,[15–17)] and back pain (22%) and emotional distress (14%)[18)] may be experienced.

To accurately depict a target surface that has curves, the envelope method[19)] and the range point migration (RPM) method[20,21)] have been proposed. These methods use a bi-static imaging technique, where the receive position is set o be different from the transmit position, and they transmit ultrasound or electromagnetic waves of hemispherical shapes. They use an ellipse, which is determined by the path length and the transmitted and received positions, to show a

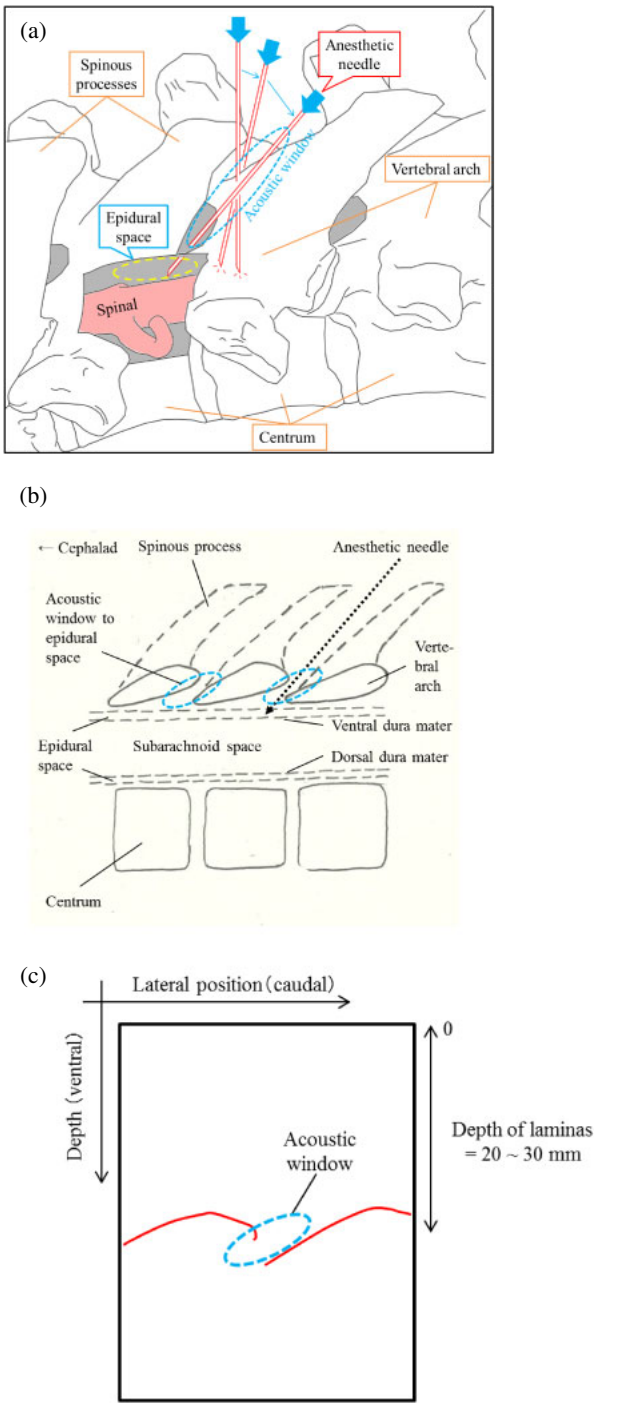

Fig. 1. (Color online) Illustrations for depicting the surface of thoracic vertebrae by ultrasound. (a) Schema of epidural anesthesia. (b) Longitudinal cross section. (c) Visualization target in cross section by ultrasound.

target surface which is tangential to the ellipse. Moreover, they depict plural ellipses which consist of a combination of many points of transmit and receive positions. These methods are characterized by high performance in rendering the target surface when a single target exists in the region of interest (ROI); however, when plural targets exist in the ROI, the estimated target surface is shallower than the actual surface, severely deteriorating the performance of these methods.

A new imaging method is herein proposed by which the vertebral surface in the thoracic area is depicted using received radio frequency (RF) data at each element of an ultrasonic probe. In the proposed method, the signal to noise ratio is improved in comparison with the conventional envelope method by employing a narrow transmit beam to reduce the number of reflected echoes from plural targets. The proposed method depicts the target surface even when targets are close to each other and has potential to be of assistance to an inexperienced examiner in administering epidural anesthesia in the thoracic area.

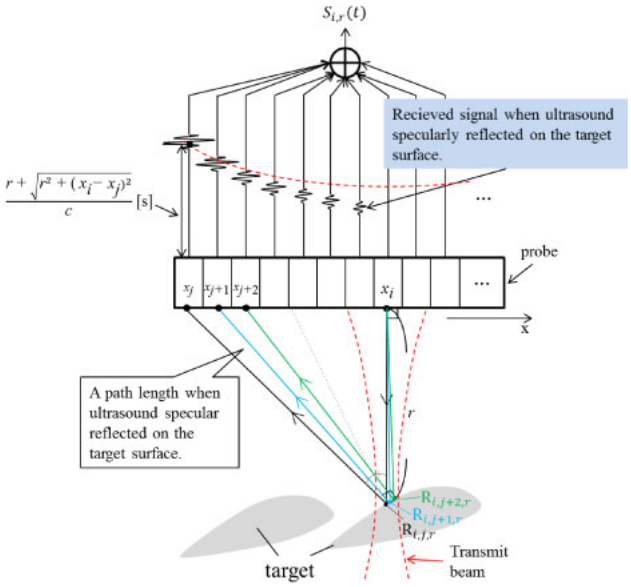

Fig. 2. (Color online) Schema of conventional B-mode imaging method.

2. Experimental methods

Figure 1(a) shows the process of epidural anesthesia in which the anesthetic needle is tapped. Since spinous processes extend caudally, an examiner inserts the anesthetic needle into the epidural space in a lateral direction to avoid these processes. Figure 1(b) depicts a paramedian section of vertebrae in the thoracic area. The aim of the present study was to depict the acoustic window between vertebral arches in the thoracic area by using ultrasound, as shown in Fig. 1(c). In an in vivo experiment, the ultrasound image of the thoracic vertebrae depicted by the proposed method was compared with a conventional B-mode image, showing the superiority of the proposed method.

2.1 Conventional B-mode imaging

Figure 2 shows a schema of conventional B-mode imaging method using a linear probe. The output signal $S_{i,r}(t)$ of the probe for observation point $R_{i,r}$ located at a distance of r along the i-th scan beam is given by the delayed sum of the received RF signals $\{s_{i,j}(t)\}$ of each element in the ultrasound probe, that is,

$$S_{i,r}(t) = \sum_j s_{i,j}\left[t + \frac{r + \sqrt{r^2 + (x_i - x_j)^2}}{c} - \frac{2r}{c}\right], \quad (1)$$

where x_i and x_j are, respectively, the lateral positions of the i-th transmit beam and the j-th received element, $s_{i,j}(t)$ is the signal received by the j-th element in response to the ultrasound transmission along the i-th scan line, and c is the acoustic velocity.

However, since conventional B-mode imaging assumes that the reflected direction from the object coincides with the incident direction on the object and since the delay values in

Eq. (1) are predesigned based on this assumption, it is difficult to obtain a high intensity when the echo comes from an inclined specular reflector, as shown in Fig. 2, resulting in low brightness of a inclined specular target surface, such as a vertebral surface.

2.2 Conventional envelope method

In the present study, the proposed method employs bi-static data acquisition as follows: In the conventional envelope method,[19] an ultrasound pulse is transmitted spherically from an element, and echoes from targets are acquired separately at each element of a probe, as shown in Fig. 3(a). The length of the path from the transmit-position X_i to the receive-position X_j is determined by summation of the lengths $\overline{X_iP_i}$ and $\overline{P_iX_j}$. Therefore, the reflection point on a target surface should be located on an ellipse, the foci of which are at the positions of X_i and X_j and the long axis of which has the same length as the path length $\overline{X_iP_i} + \overline{P_iX_j}$.

By scanning the transmitted position X_i along the probe, the conventional envelope method depicts plural ellipses which consist of many points of transmit position X_i and receive position X_j, and finally estimates the target surface as the outer envelope of the ellipses. However, when there are plural targets in the ROI, the target surface estimated by the conventional envelope method is restricted to a shallow depth, as shown in Fig. 3(a). Since the method selects one receive-position X_j from all positions $\{X_j\}$, the path length $\overline{X_iP_i} + \overline{P_iX_j}$ has a minimum. Thus, position $X_{j'}$ is selected but X_j and $X_{j''}$ are not, as shown in Fig. 3(b).

2.3 Proposed method with limited width and direction of transmit beam

A modified envelope method by limiting the width and direction of the transmit beam, as shown in Fig. 3(c), is herein proposed. In the proposed method, a narrow transmit beam rather than a spherical beam is employed. Alternatively, the transmitted beam is set to be inclined by θ. For the resultant plural ellipses which consist of many points of transmit position X_i and receive position X_j, the arc of each ellipse is employed only within the width of the transmit beam. The grid size is 56 and 50 mm in the lateral and depth directions, respectively. The compound image is constructed by the summation of several images depicted by the proposed method using various incident angles $\{\theta\}$ of the transmit beam. Thus, the proposed method restricts the number of assumed targets that reflect ultrasound and can depict ellipses in the area of a gap. Moreover, in the proposed method, the received signal intensity acquired by the narrow transmit beam is greater than that acquired by the spherical beam. Therefore, the proposed method can obtain signals on deeper target surfaces.

2.4 In vivo experiment of thoracic vertebrae

RF signals of each element in the ultrasonic probe were acquired for the thoracic vertebrae of a healthy 23-year-old male using an ultrasound diagnostic device (Prosound alpha 10, Hitachi-Aloka). The resultant image obtained by the proposed method was compared with a conventional B-mode image. The employed linear array probe consisted of 192 elements with an element pitch of 0.2 mm. The transmit frequency, sampling frequency, and focal distance were 7.5 MHz, 40 MHz, and 30 mm, respectively. The inclined angle of transmit beam θ ranged from -20 to 20°, the angle interval being 5°.

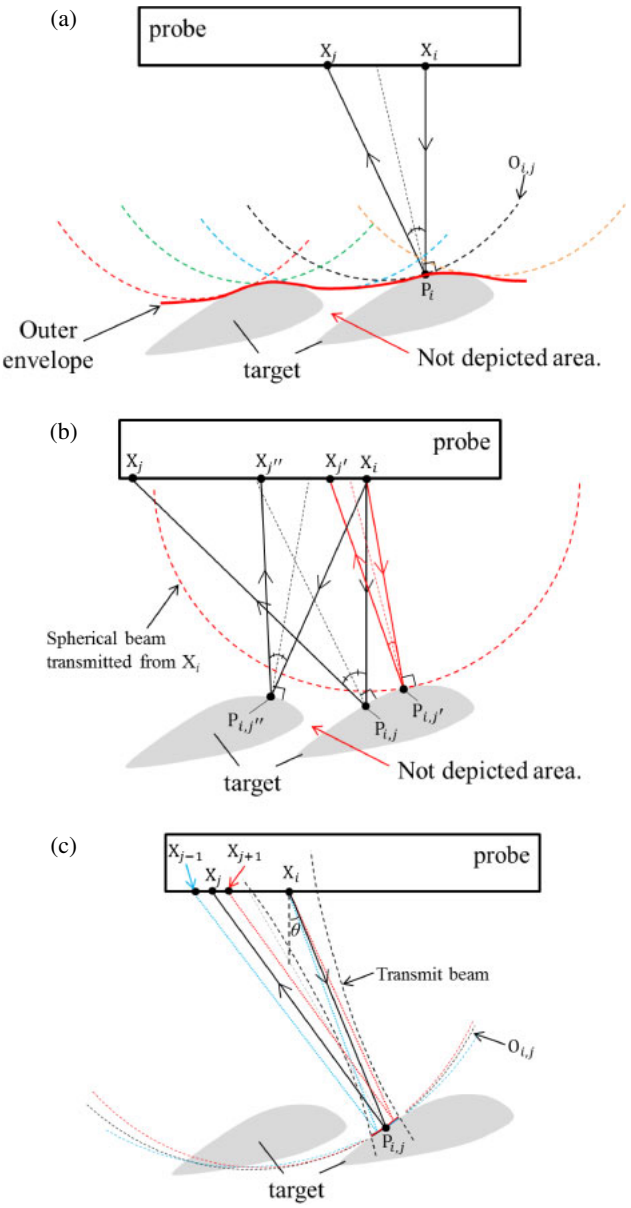

Fig. 3. (Color online) (a, b) Schemas of the conventional envelope method. In the conventional envelope method, the path length $\overline{X_iP_{i,j'}} + \overline{P_{i,j'}X_{j'}}$ which is the shortest in (b) is selected. (c) Schema of the proposed method with limited width and direction of the transmit beam.

3. Results

Figure 4(a) illustrates the vertebral surface and muscle tissue on a conventional B-mode image. Figure 4(b) shows the B-mode image of the thoracic vertebral surface. Figure 4(c) shows the signal power of the echoes from the vertebral surface and muscle tissue with respect to the various transmit beam directions $\{\theta\}$, where ten measurement positions were assigned, as shown in Fig. 4(b). The echoes from the vertebral surface were higher in intensity compared with those from the muscle tissue.

Figures 5(a)–5(i) show the images obtained by the proposed method. Especially when transmit beam direction θ was 15° in Fig. 5(h) or 20° in Fig. 5(i), the proposed method clearly depicted the vertebral surface without an effect of the muscle tissue as compared with the conventional B-mode image in Fig. 4(b).

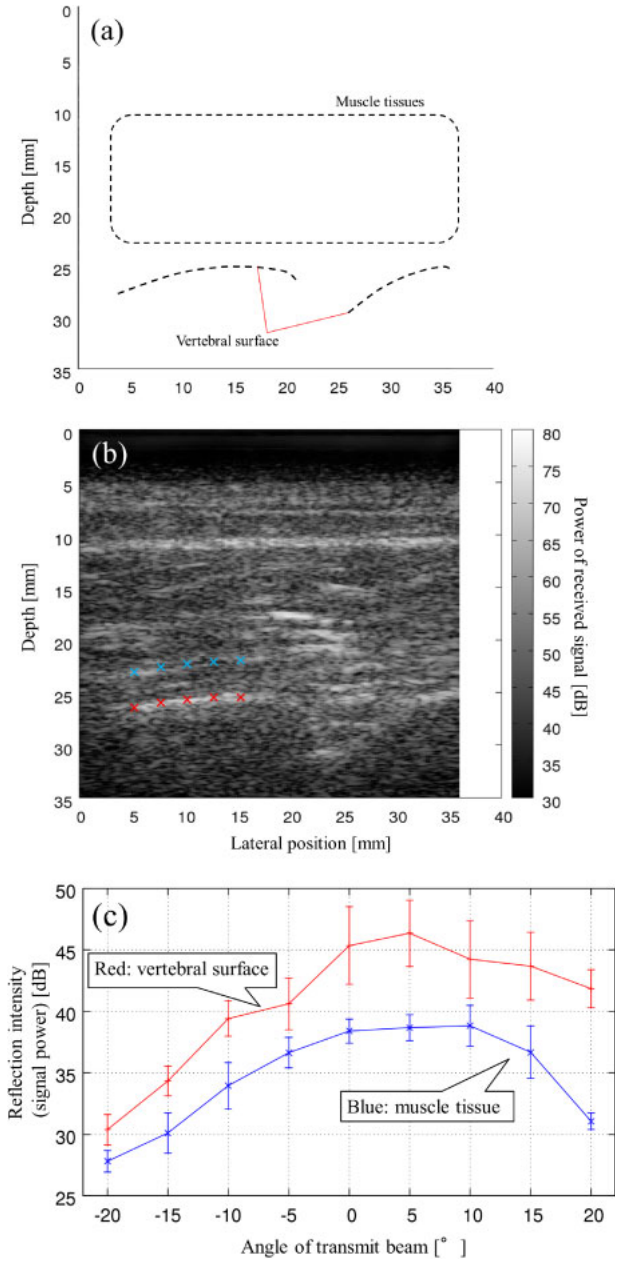

Fig. 4. (Color online) (a) Vertebral surface and muscle tissue assumed on B-mode image. (b) Conventional B-mode image of the surface of thoracic vertebrae. Crosses show the assigned points on the vertebral surface (red) and muscle tissue (blue). (c) The received power depends on the inclined angle θ of the transmitted beam. (The reflected angle coincides with the incident angle.)

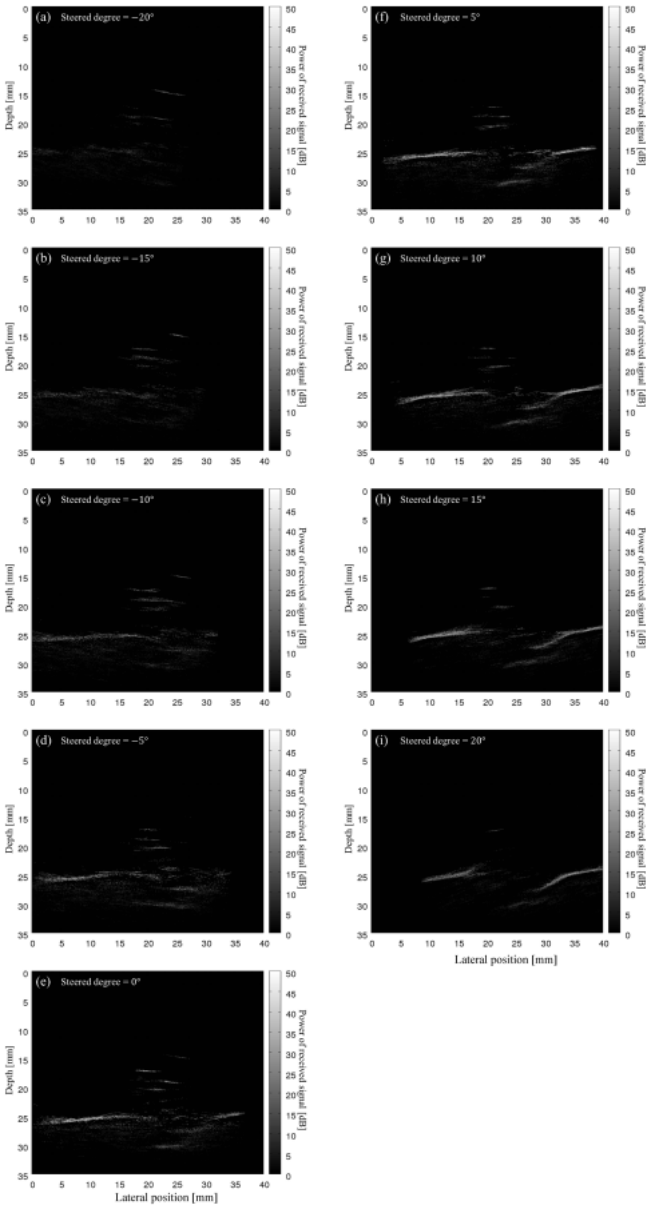

Fig. 5. Surface of the thoracic vertebrae estimated by the proposed method using width and direction of the transmit beam. The results when the transmit beam angle is −20, −15, −10, 0, 5, 10, 15, 20° from (a) to (i), respectively.

Figure 6(a) shows a conventional B-mode image of the thoracic vertebral surface. In the B-mode image, the vertebral surface at depth of about 26 mm was depicted, but the influence due to the muscle tissue at depths from 10 to 23 mm was not negligible.

Figure 6(b) shows the images obtained by the conventional envelope method. In this method, a narrow transmit beam was employed. The red line shows the outer envelope, which is tangential to the depicted plural ellipses. This method estimates the vertebral surface at a shallow depth because it selects the shortest path length as the long axis of an ellipse.

Figure 6(c) shows a compounded image of Figs. 5(a)–5(i), the images obtained by the proposed method. In the compounded result, the vertebral surface was depicted as being smoother than that of each angle result of Fig. 5 acquired by the proposed method. The white boxes in Figs. 6(a) and 6(b) show the assigned area of the vertebral surface and muscle tissue. Inside each box, the average power was calculated and the contrast ratio defined by the ratio of the power in the vertebral surface area to the power in the muscle tissue area was calculated. The contrast ratio was 10.2 dB in Fig. 6(a) and 31.1 dB in Fig. 6(b). Thus, the proposed method was able to more clearly depict the vertebral surface than possible with conventional B-mode imaging.

4. Discussion

A clearer image was obtained by the proposed method than by the B-mode imaging method. This result shows that the measurement plane was not perpendicular to the vertebral

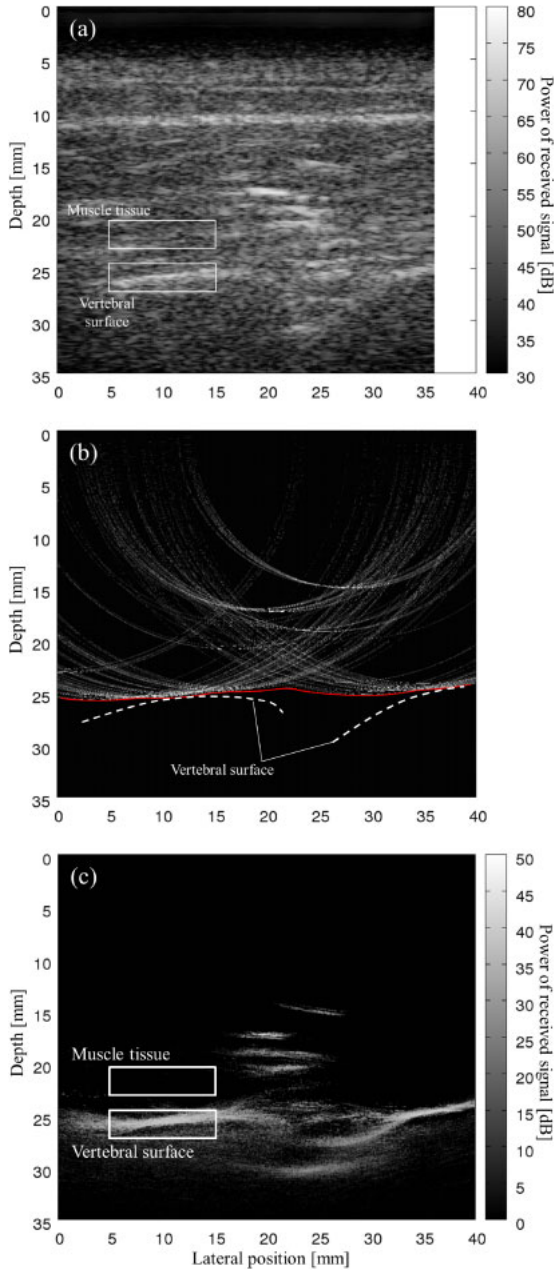

Fig. 6. (Color online) (a) Conventional B-mode image for the thoracic vertebral surface. (b) Surface of the thoracic vertebrae estimated by the conventional envelope method. The red line shows the outer envelope as the estimated vertebral surface. (c) Surface of the thoracic vertebrae estimated by the proposed method. The results of all angles are compounded. The white boxes show the assigned area of the vertebral surface and that of the muscle tissue.

surface, as shown Fig. 4(c), which may also occur in clinical practice because of the difficulty of vertical access to the vertebral surface. Even though this condition exists in the proposed method, this method was successful in depicting the vertebral surface. This shows the robustness of the visualization of the vertebral surface by the proposed method.

The proposed method selectively depicts the vertebral surface with the suppression of the contribution of soft tissue. This study intended to localize the gap between vertebrae by the clear depiction of the thoracic vertebral surface. Therefore, the suppression of the contribution of soft tissue will facilitate administration of thoracic anesthesia by the accurate depiction of the vertebral surface.

The frame rate of the proposed method is about 1/9 of the conventional B-mode imaging method because nine images are used to acquire a compound image. Since the movement due to the heartbeat is imperceptible in the practice of thoracic anesthesia, the proposed method is useful for the observation and localization of the vertebral surface.

5. Conclusions

Herein, we proposed an envelope method with limited width and direction of the transmit beam, depicted the surface of the thoracic vertebrae in vivo, evaluated the ability of depiction and compared the results of this method with B-mode imaging. From the results of this study, it was shown that the proposed method can clearly and extensively depict the vertebral surface. As explained above, the possibility was suggested that the proposed method is suitable as an auxiliary technique for visualization of the vertebral surface to safely achieve epidural anesthesia.

1) M. J. Osterman and J. A. Martin, Natl. Vital Stat. Rep. **59** [5], 1 (2011).
2) H. Niinai, I. Nakagawa, H. Hamada, A. Sakai, M. Kimura, and M. Yasuuji, Masui **48**, 295 (1999) [in Japanese].
3) R. D. Miller, L. I. Eriksson, L. A. Fleisher, J. P. Wiener-Kronish, N. H. Cohen, and W. L. Young, *Miller's Anesthesia* (Saunders, Amsterdam, 2015).
4) Y. Sakai, H. Taki, and H. Kanai, Jpn. J. Appl. Phys. **55**, 07KF11 (2016).
5) Y. Kurokawa, H. Taki, S. Yashiro, K. Nagasawa, Y. Ishigaki, and H. Kanai, Jpn. J. Appl. Phys. **55**, 07KF12 (2016).
6) Y. Mochizuki, H. Taki, and H. Kanai, Jpn. J. Appl. Phys. **55**, 07KF13 (2016).
7) Y. Miyachi, H. Hasegawa, and H. Kanai, Jpn. J. Appl. Phys. **54**, 07HF18 (2015).
8) M. Yamauchi, Trends Anaesth. Crit. Care **2**, 234 (2012).
9) I. Hacihaliloglu, R. Abugharbieh, A. J. Hodgson, and R. N. Rohling, Ultrasound Med. Biol. **35**, 1475 (2009).
10) S. Yu, K. K. Tan, B. L. Sng, S. Li, and A. T. H. Sia, Ultrasound Med. Biol. **40**, 1980 (2014).
11) B. Kerby, R. Rohling, V. Nair, and P. Abolmaesumi, Proc. 30th Annu. Int. Conf. IEEE Engineering in Medicine Biology Society, 2008, p. 2980.
12) D. Tran and R. N. Rohling, IEEE Trans. Biomed. Eng. **57**, 2248 (2010).
13) T. Komatsu, Y. Satoh, G. Shirakami, N. Seo, and K. Hirota, *Choonpa Gaidoka Sekichukan/Bosekitsui Block* (Ultrasound-Guided Spinal Canal and Paravertebral Block) (Kokuseido, Tokyo, 2011) p. 14 [in Japanese].
14) T. Grau, R. W. Leipold, S. Delorme, E. Martin, and J. Motsch, Reg. Anesth. Pain Med. **27**, 200 (2002).
15) C. Konrad, G. Schupfer, M. Wietlisbach, and H. Gerber, Anesth. Analg. **86**, 635 (1998).
16) G. Le Coq, B. Ducot, and D. Benhamou, Can. J. Anaesth. **45**, 719 (1998).
17) M. P. N. Lewis, P. Thomas, L. F. Wilson, and R. C. Mulholland, Anesth. Analg. **47**, 57 (1992).
18) *Complications of Regional Anesthesia*, ed. B. Finucane (Springer, New York, 2009) 2nd ed., p. 441.
19) T. Sakamoto, H. Taki, and T. Sato, Acoust. Sci. Technol. **32**, 143 (2011).
20) S. Kidera, T. Sakamoto, and T. Sato, IEEE Trans. Geosci. Remote Sens. **48**, 1993 (2010).
21) H. Taki, S. Tanimura, T. Sakamoto, T. Shiina, and T. Sato, J. Med. Ultrason. **42**, 51 (2015).